European Radiology
https://doi.org/10.1007/s00330-022-08608-7

VASCULAR-INTERVENTIONAL

Morphology-aware multi-source fusion–based intracranial aneurysms rupture prediction

Chubin Ou[1,2] · Caizi Li[3] · Yi Qian[1] · Chuan-Zhi Duan[1] · Weixin Si[3] · Xin Zhang[1] · Xifeng Li[1] · Michael Morgan[2] · Qi Dou[4] · Pheng-Ann Heng[4]

Received: 12 September 2021 / Revised: 29 December 2021 / Accepted: 23 January 2022

Abstract

Objectives We proposed a new approach to train deep learning model for aneurysm rupture prediction which only uses a limited amount of labeled data.

Method Using segmented aneurysm mask as input, a backbone model was pretrained using a self-supervised method to learn deep embeddings of aneurysm morphology from 947 unlabeled cases of angiographic images. Subsequently, the backbone model was finetuned using 120 labeled cases with known rupture status. Clinical information was integrated with deep embeddings to further improve prediction performance. The proposed model was compared with radiomics and conventional morphology models in prediction performance. An assistive diagnosis system was also developed based on the model and was tested with five neurosurgeons.

Result Our method achieved an area under the receiver operating characteristic curve (AUC) of 0.823, outperforming deep learning model trained from scratch (0.787). By integrating with clinical information, the proposed model's performance was further improved to AUC = 0.853, making the results significantly better than model based on radiomics (AUC = 0.805, p = 0.007) or model based on conventional morphology parameters (AUC = 0.766, p = 0.001). Our model also achieved the highest sensitivity, PPV, NPV, and accuracy among the others. Neurosurgeons' prediction performance was improved from AUC=0.877 to 0.945 (p = 0.037) with the assistive diagnosis system.

Conclusion Our proposed method could develop competitive deep learning model for rupture prediction using only a limited amount of data. The assistive diagnosis system could be useful for neurosurgeons to predict rupture.

Key Points

- *A self-supervised learning method was proposed to mitigate the data-hungry issue of deep learning, enabling training deep neural network with a limited amount of data.*
- *Using the proposed method, deep embeddings were extracted to represent intracranial aneurysm morphology. Prediction model based on deep embeddings was significantly better than conventional morphology model and radiomics model.*
- *An assistive diagnosis system was developed using deep embeddings for case-based reasoning, which was shown to significantly improve neurosurgeons' performance to predict rupture.*

Chubin Ou and Caizi Li contributed equally to this work.

✉ Yi Qian
yi.chien.qian@gmail.com

✉ Chuan-Zhi Duan
doctor_duanzj@163.com

✉ Weixin Si
wx.si@siat.ac.cn

[1] Neurosurgery Center, Department of Cerebrovascular Surgery, The National Key Clinical Specialty, The Engineering Technology Research Center of Education Ministry of China on Diagnosis and Treatment of Cerebrovascular Disease, Guangdong Provincial Key Laboratory on Brain Function Repair and Regeneration, The Neurosurgery Institute of Guangdong Province, Zhujiang Hospital, Southern Medical University, Guangzhou, Guangdong, China

[2] Faculty of Medicine and Health Sciences, Macquarie University, Sydney, New South Wales, Australia

[3] Shenzhen Institute of Advanced Technology, Chinese Academy of Sciences, Shenzhen, China

[4] Department of Computer Science and Engineering, The Chinese University of Hong Kong, Shatin, Hong Kong SAR

Published online: 18 February 2022

Keywords Stroke · Aneurysm rupture · Self-supervised training · Deep embeddings · Computer-aided diagnosis

Abbreviations

AUC Area under the receiver operating characteristic curve
CTA Computed tomography angiography
DSA Digital subtraction angiography
MRA Magnetic resonance angiography

Introduction

Intracranial aneurysms (IA) are present in 3–7% of the population [1]. Though the annual rupture rates of aneurysms are usually below 1%, the rupture of aneurysms can cause lethal event such as subarachnoid hemorrhage (stroke), leading to a mortality rate as high as 65% [2–4]. Surgical or endovascular treatments for aneurysm repair still carry a significant risk of complications [3]. Therefore, aneurysm rupture prediction and stratification of patients according to the risk of rupture would facilitate the management of IA and lead to better outcome. Various factors have been suggested to be associated with rupture, such as aneurysm size, morphology, hemodynamics [5–10], hypertension [11], blood lipid level [12], alcohol consumption, and smoking [13–15]. Based on these risk factors, various risk evaluation methods have been proposed. The PHASES score is among the most quoted one [16], which calculates rupture risk based on aneurysm size, location, age, ethnicity, and previous subarachnoid hemorrhage history. However, the prediction performance (AUC = 0.66 ~ 0.76) still needs to be improved [17].

Shi et al presented a detailed review of artificial intelligence applied in the research area of intracranial aneurysms [18]. Deep neural network has been applied in the detection of aneurysm from MRA images [19–23], CTA images [24–26], and DSA images [27]. In the research area of rupture prediction, most studies employ logistic regression [v,vi]. Some used classic machine learning algorithms such as support vector machine and random forest, with features such as morphology [28], hemodynamics [29], radiomics [30, 31], and clinical information [32] as input variables.

Deep learning models are usually more powerful than statistical learning models as deeper network can extract more intrinsic and complex features and relations from data. However, few studies reported using deep learning for rupture prediction [33, 34]. There is also one study using deep learning to predict the occurrence of aneurysm [35]. Deep learning models typically require large number of cases for training purposes. The performance of deep learning models was found to be related to the amount of training data [26].

Unfortunately, there are some clinical areas where it is difficult to obtain a large amount of labeled data. For example, it is often difficult to collect a large number of untreated aneurysm cases with acceptable image quality and sufficiently long follow-up period. This is because most unruptured aneurysm presented to hospital will be treated. Most ruptured cases only have post-rupture images, whose morphology differs significantly from their pre-rupture state [36]. For rupture prediction purpose, pre-rupture images should be used instead of post-rupture images. As obtaining aneurysm images with sufficiently long follow-up is often very difficult, most of the studies mentioned above developed their model based on retrospective and cross-sectional data, which may limit their applicability. A limited amount of data may also hamper the performance of deep neural network.

There are several large prospective cohort studies in the past [37, 38]. However, imaging data of such studies were not made public. There are some publicly available aneurysm databases with angiographic imaging data [39, 40]. However, the rupture status of aneurysms in these datasets is either unknown or is cross-sectional data without follow-up.

In this paper, we aimed to predict the 2-year rupture risk of untreated aneurysm with follow-up data. We proposed a novel approach to train deep learning models with only a limited amount of data: a self-supervised learning framework to perform pre-training on a large amount of unlabeled data, aiming to extract deep embeddings (features) to represent aneurysm morphology. We further fused clinical information with the deep embeddings for improved performance. To further demonstrate the effectiveness of our proposed method, we developed a computer-aided system featuring case-based reasoning. We tested the system with five neurosurgeons, showing significantly improved surgeons prediction performance.

Methods

Description of datasets

In the following context, we referred to labeled data as aneurysm cases with known rupture/stable status during follow-up. We referred to unlabeled data as aneurysm cases whose rupture status was unknown or aneurysm cases without follow-up (cross-sectional data). Unlabeled data are much easier to collect and exist in large amounts. In contrast, labeled data (follow-up cases) are much fewer.

This study was approved by the local institution ethics committees and patients' informed consent was obtained. Aneurysm cases were collected from our database between 2008 and 2020. The selection criteria included a confirmed diagnosis of one or more intracranial aneurysms. Cases with incomplete record of follow-up, cases treated immediately after diagnosis, or cases with insufficient image quality were

Table 1 Baseline characteristics of ruptured and stable aneurysms

	Ruptured (29)	Stable (91)	*p*
Age	54.20 ± 13.10	55.75 ± 10.37	0.513
Female	12	60	0.566
Size (mm)	9.73 ± 7.55	5.07 ± 3.01	< 0.001
Neck width (mm)	5.23 ± 2.32	4.27 ± 1.48	0.01
Parent artery diameter (mm)	2.73 ± 0.68	3.09 ± 0.82	0.038
Size ratio	3.61 ± 2.67	1.72 ± 1.01	< 0.001
Aspect ratio	2.03 ± 1.88	1.19 ± 0.53	< 0.001
Type (bifurcation)	16	32	0.055
Irregular shape	10	17	0.076
Location			0.027
ICA	5	34	
MCA	11	22	
PComA	4	20	
AComA/ACA	6	12	
Posterior Circ	3	3	

excluded. In the current study, stable aneurysms were defined as aneurysms which remained unruptured and asymptomatic for at least 2 years during follow-up. Ruptured aneurysms were defined as aneurysms who ruptured during yearly follow-up. Since aneurysm morphologies may differ significantly before and after rupture, only the pre-rupture images were used. For patients having multiple follow-up image series, only the earliest series was used. Ninety-nine cases containing 120 aneurysms (91 unruptured, 29 ruptured) with CTA images were selected. We refer to these cases with known stable/rupture status as labeled data. The baseline characteristics of the labeled cases are shown in Table 1.

We also collected aneurysm cases from multiple sources including other hospitals' databases and online databases. However, these cases either do not have rupture status information available or are unruptured aneurysms treated immediately, or are ruptured aneurysms with only post-rupture images. Therefore, such cases are not suitable for building a rupture prediction model. We refer to such cases as unlabeled cases. In total, 132 cases (144 aneurysms) in DSA format and 325 cases (488 aneurysms) in CTA format were collected from two hospitals' database. One hundred and thirty-one cases (157 aneurysms) in DSA imaging were collected from the online database (CADA - Aneurysm Detection Challenge). Ninety-three cases (158 aneurysms) in MRA imaging were collected from online database (ADAM - Aneurysm Detection and Segmentation Challenge). Therefore, a total of 947 aneurysms were used as unlabeled cases, as shown in Table 2. These cases were used to pretrain our network. All images were resampled to have equal spacing (0.5 mm * 0.5 mm * 0.5 mm) and sub-volume containing the aneurysm sac (size, 32 mm * 32 mm * 32 mm) were extracted from the original volume. For aneurysms from online databases, the official segmentation result was used. For aneurysms from hospitals, they were manually segmented using 3D Slicer (https://www.slicer.org/). Cases collected from hospitals cannot be made public at the moment due to ethics approval.

Table 2 Summary of unlabeled data

Source	Modality	Number of aneurysms
Hospitals	DSA	144
Hospitals	CTA	488
CADA public database	DSA	157
ADAM public database	MRA	158
Total		947

Training method and network architecture

Methodology design motivation

Conventional morphology features may not fully represent the complex morphology of aneurysm. Therefore, in this study, we focused on extracting morphology-aware deep embeddings of aneurysms. We believed that a better representation (embeddings) of morphology can help improve the accuracy of rupture prediction.

Overview of the proposed method

The overall pipeline of our proposed method has been presented in Figure 1. First, we proposed a self-supervised learning framework to make full use of large-scale unlabeled aneurysm cases. A backbone network of a 3D ResNet18 followed by a fully connected layer was pretrained using the unlabeled aneurysm cases to extract deep embeddings (features of 64 channels) of aneurysm morphology. ROIs of size 64 × 64 × 64 containing aneurysm segmentation binary mask were cropped from the original image volume and used as input to feed the neural network. The pretrained network was then finetuned using the 120 labeled cases. Two extra fully connected layers were added after the backbone network to output the rupture probability. The designs of the learning framework and network architecture are shown on the right side of Figure 1. For technical details of the methodology, please refer to the supplementary material. The source code of https://github.com/CaiziLee/Aneurysms_Rupture_Prediction.

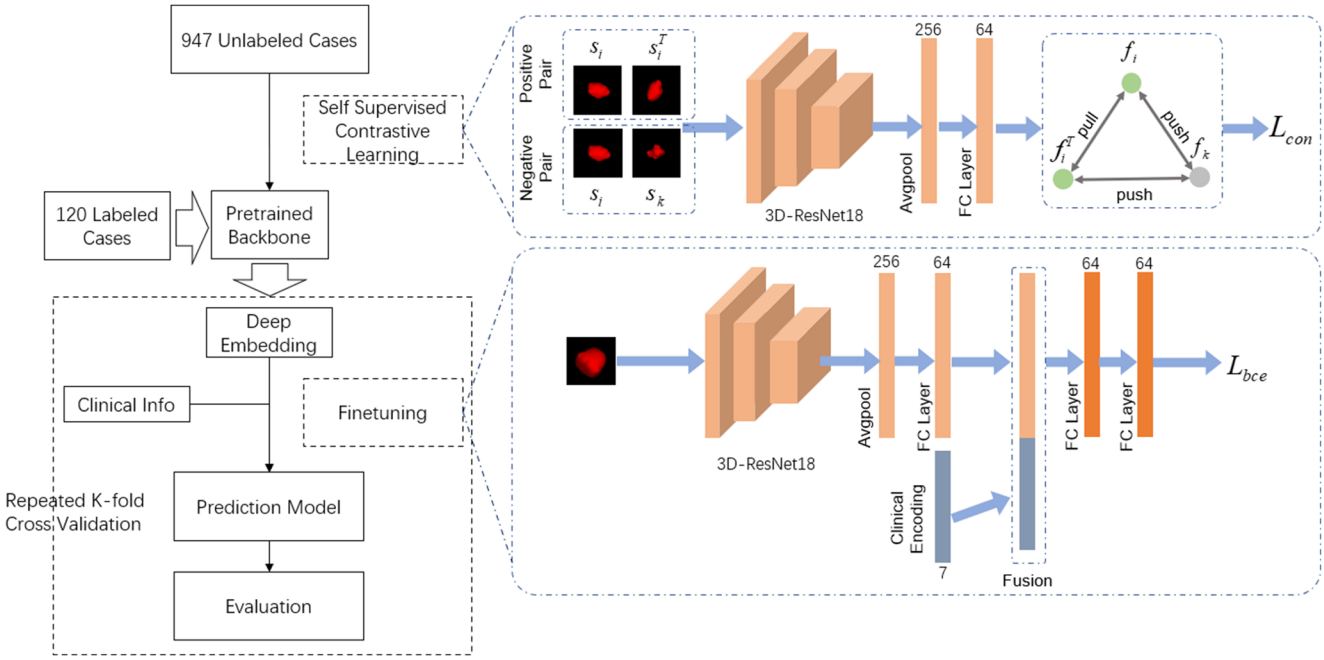

Fig. 1 Overall pipeline of the proposed method

Evaluation of model performance

To reduce overfitting and increase the confidence in our result, we performed a repeated *k*-fold cross-validation, which has been proved to be stable and representative even for a small dataset [41]. In each repeat of the cross-validation process, the data was split into five folds. Four folds were used as training set and the remaining one fold was used as a test set to evaluate the model performance. The process repeats until each fold has been used as the test set for once. The above cross-validation process was repeated for 5 times and each time with a different split of training data and test data. For details of the cross-validation process, please see Supplemental Material and Supplemental Figure 1. The average performance in the five tests was reported.

To demonstrate the competency of our model, we first compared our method with classical regression model. The regression model was developed using morphology (size, size ratio, aspect ratio, location, saccular/bifurcation) and clinical information (gender, age, multiplicity). Radiomics has recently been shown to be able to predict rupture [30, 31]; therefore, we further compared our method with a model developed using radiomics shape features and clinical information. We also compared our method with a deep learning model trained from scratch to demonstrate the importance of self-supervised pretraining. Similarly, all competing models were evaluated using repeated fivefold cross-validation.

Development of assistive diagnosis system with case-based reasoning

To demonstrate the clinical applicability of our model, we further developed a computer-aided risk assessment system. The system took an aneurysm's image and clinical information as input and output the corresponding rupture probability. The user was provided with a user interface showing the 3D shape of aneurysm, clinical information, and rupture probability on the left side. To provide extra supporting information for decision making, we designed a deep embedding empowered case-based reasoning approach in our system. Supporting example aneurysms that were morphologically similar were extracted from database. The similarity of two aneurysms' morphology was evaluated by the Euclidian distance between the two embeddings obtained from self-supervised pretraining. After the supporting example aneurysm was extracted, its 3D shape, clinical information, and rupture status were displayed next to the examined aneurysm, as shown in Figure 2. The supporting example aneurysm was aimed to provide extra information support to neurosurgeons and allow them to make decision by case-based reasoning.

Clinical test of the proposed system

To test the clinical applicability of the system, the pretrained model was finetuned using 96 cases while the rest of the 24 cases were held out for testing. Five neurosurgeons, who were blinded to the rupture status of the 24 cases, were recruited for the test. The years of experience of the five neurosurgeons

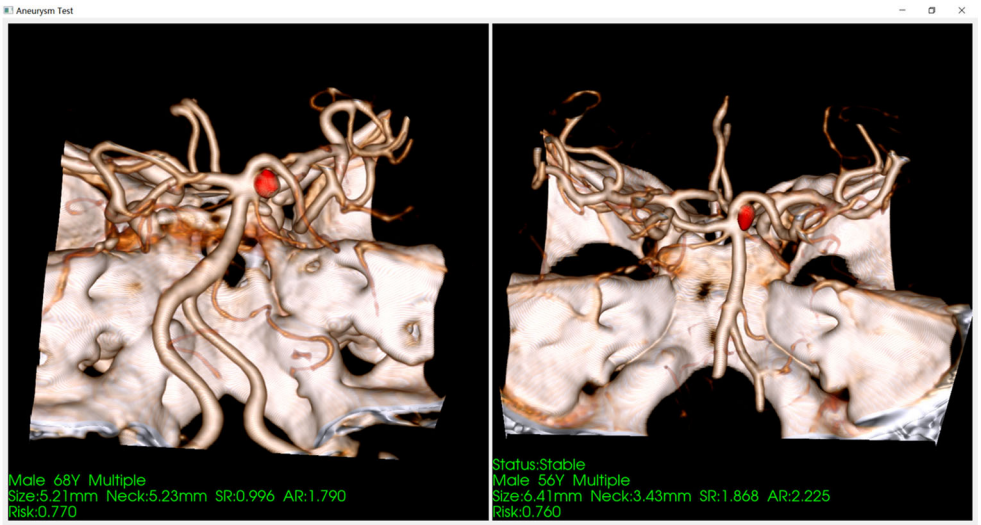

Fig. 2 User interface of the computer-aided diagnosis system. Left window shows the aneurysm being examined. Right window shows example aneurysm extracted from database. The bottom shows the clinical information and estimated rupture risk

were 2, 4, 5, 8, and 12. In the first test, the system was run without showing the supporting example aneurysm. Neurosurgeons were only provided with the 3D images of aneurysm being examined, clinical information, and the predicted rupture probability from the model. They were asked to grade these cases for rupture risk in a scale of 1 to 10, with 10 being the highest risk. After a 2-week wash-out period, the neurosurgeons were asked to grade the same 24 cases again. In the second test, besides the information provided in the first test, they were also provided with extra information: supporting example aneurysm extracted from the database. The performance of the neurosurgeons in the two tests was evaluated by the area under the receiver operating characteristic curve (AUC), sensitivity, and specificity using a cutoff value of 5.

Statistical analysis

The performance differences of neurosurgeons in the two tests (with/without the supporting example) were assessed by paired the Student *t*-test. The Benjamini-Hochberg correction was used to correct for multiple comparison: an adjusted $p \leq 0.05$ indicated statistical significance. For comparison of the repeated *k*-fold cross-validation performance, Wilcoxon signed-ranks test was used as suggested in previous study [42].

Results

Comparison of performance with competing methods

The averaged AUC, accuracy, sensitivity, specificity, PPV, and NPV of different methods are presented in Table 3. Conventional regression model achieved an AUC of 0.766. Radiomics model achieved a higher AUC of 0.805. Our proposed method (C) achieved the best performance of 0.853, which was significantly better than the morphology-based regression model ($p = 0.001$) and radiomics-based regression model ($p = 0.007$). Our proposed method also achieved the

Table 3 Comparison of performance with competing method

Method	AUC	Sensitivity	Specificity	PPV	NPV	Accuracy
A	0.787 ± 0.035	0.803 ± 0.051	0.742 ± 0.015	0.513 ± 0.021	0.914 ± 0.015	0.786 ± 0.015
B	0.823 ± 0.033	0.886 ± 0.021	0.801 ± 0.020	0.563 ± 0.023	0.934 ± 0.016	0.800 ± 0.015
C	0.853 ± 0.025	0.893 ± 0.031	0.838 ± 0.026	0.692 ± 0.039	0.967 ± 0.010	0.853 ± 0.016
D	0.805 ± 0.016	0.865 ± 0.029	0.687 ± 0.027	0.488 ± 0.022	0.951 ± 0.010	0.785 ± 0.007
E	0.766 ± 0.019	0.806 ± 0.038	0.697 ± 0.034	0.508 ± 0.032	0.935 ± 0.012	0.784 ± 0.014

Note: Method A: Deep learning model trained from scratch

Method B: Self-supervised pretrain + finetuning

Method C: Self-supervised pretrain + finetuning with clinical info

Method D: Radiomics with clinical info + LASSO regression

Method E: Morphology with clinical info + LASSO regression

Table 4 Comparison of neurosurgeon performances with/without supporting examples

Metric	Test 1	Test 2	Adjusted *p*
AUC	0.877 ± 0.036	0.945 ± 0.039	0.037*
Sensitivity	0.933 ± 0.041	0.966 ± 0.033	0.089
Specificity	0.511 ± 0.106	0.633 ± 0.084	0.047*

highest sensitivity, PPV, NPV, and accuracy. This has demonstrated our method's competency over conventional methods.

Table 3 also shows the importance of our proposed self-supervised pretraining method when we compare method A and B deep learning model trained from scratch performed relatively poor (0.787) without pretraining. This was also reflected in another study [33]. The relatively poor performance is likely due to the insufficient amount of training data. Our proposed method, using self-supervised pretraining, can overcome the data-hungry issue of deep learning and improve the deep neural network performance to 0.823 (method B). By comparing methods B and C, we can see that integration with clinical information can further boost the performance.

Comparison of performance of neurosurgeons

The performance of the five neurosurgeons, with (test 2) and without (test 1) aid from supporting example aneurysm, is shown in Table 4. Significant improvements in terms of AUC (p = 0.037) and specificity (p = 0.047) were observed for neurosurgeons with aid from showing the supporting example aneurysm (test 2). Improvement of sensitivity was also observed but it did not achieve statistical significance. The inter-rater and intra-rater reliabilities of risk grading were also examined by intraclass correlation coefficient, which were 0.818 (95%CI 0.724 – 0.912) and 0.893 (95%CI 0.805 – 0.981), indicating good repeatability of the test.

Figure 3 below shows the performance change of the five neurosurgeons. Marked improvement can be seen for NS1, NS2, NS3, and NS4 in terms of AUC and specificity. NS1 and NS4 showed improvement in terms of sensitivity. NS5 performed approximately equal with or without the supporting example. In terms of AUC, most prominent improvement was seen for novice neurosurgeon (NS1). NS2, NS3, and NS4 can be improved to a similar level to the most senior neurosurgeon (NS5) with the aid of supporting example.

Figure 4 below shows three typical pairs of query aneurysms (top row) and example aneurysms (bottom row) extracted based on deep embedding distance. These example aneurysms have similar size, morphology, and surface regularity to their query counterpart. This demonstrated that deep embeddings can well capture the morphologic characteristics of aneurysms.

Discussion

In this paper, we proposed a self-supervised learning method to extract deep embeddings of aneurysm morphology for rupture prediction. Our method can accurately predict aneurysm mid-term stability within 2 years. We further developed a computer-aided diagnosis system which employed a case-based reasoning approach based on deep embeddings of aneurysms. The system was tested with five neurosurgeons at different levels and significant improvement was observed for their performance in predicting aneurysm rupture.

Assessing rupture risk of aneurysms has been an active research area for many years. In recent years, artificial intelligence, the predominantly statistical learning method, has been applied to develop model for rupture prediction. In contrast, though deep learning has been widely used in aneurysm detection [19-25], few studies have used deep learning to assess rupture risk and reported only limited performance [33, 34]. One of the reasons may lie in the small training sample size as

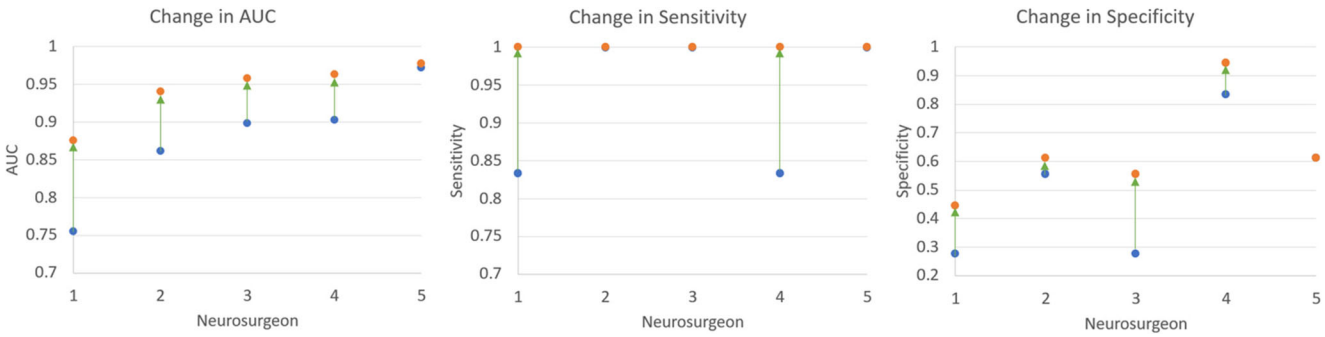

Fig. 3 Performance change of neurosurgeons with/without showing supporting example aneurysm. Blue dots represent the performance without the supporting example (test 1). Orange dots represent the performance with supporting example (test 2). When there is no gain of performance, only the orange dot is shown

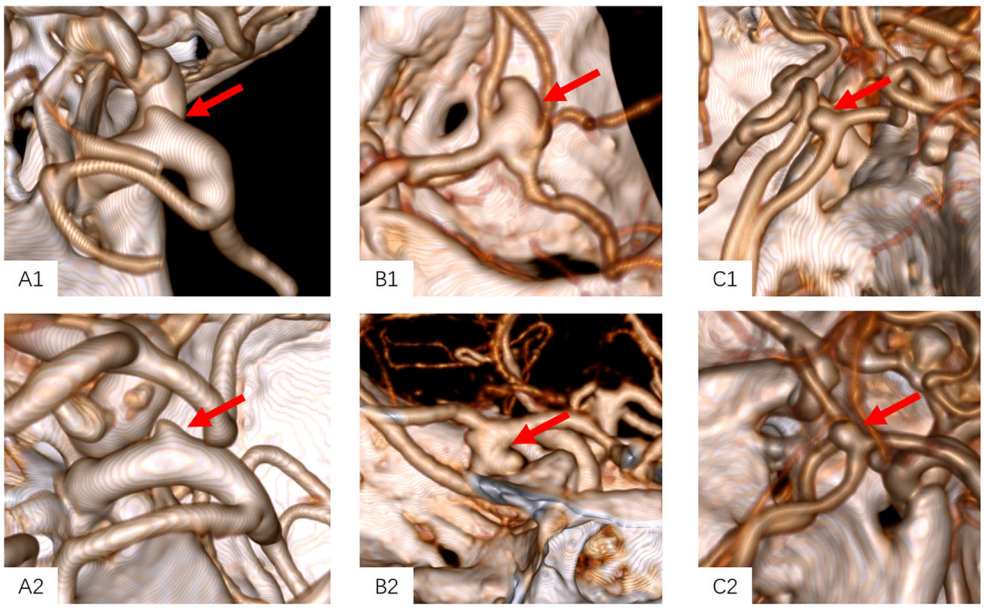

Fig. 4 Typical supporting example aneurysm extracted from the database. The top row shows the query aneurysms being examined. The bottom row shows the supporting example aneurysm extracted by the system. **A1** and **A2** are both located on ICA, with similar sizes of 2.15mm and 1.96mm, respectively. **B1** and **B2** are MCA aneurysms. Both have irregular surfaces and similar sizes of 7.44 mm and 6.12 mm, respectively. **C1** and **C2** are AComA aneurysms. Both feature slight bulging of the communicating branch on AComA and similar sizes of 3.81 mm and 3.31 mm

deep learning models typically require a very large sample size to train, which is often difficult to collect.

To overcome the issue of insufficient training data, we proposed a self-supervised learning method to pretrain neural network using the more abundantly available unlabeled cases. Our method performed better than the supervised trained model when subject to insufficient data. Our method can also be applied to other clinical areas where data scarcity is a problem, making the data-hungry deep learning more accessible.

Most previous works predicted rupture by giving a number, such as the Rupture Resemblance Score [43], Intracranial Aneurysm Rupture Score [44], and the PHASES Score [16]. Neurosurgeons may have different interpretations of these numbers. For example, some may consider a rupture probability of 0.51 as high but some may consider the opposite. Moreover, deep learning-based model is notorious for its black-box nature, which may reduce the confidence of neurosurgeons in using such model. To alleviate this problem, we proposed a case-based reasoning approach in this paper. By exploiting the morphology-aware deep embeddings extracted from aneurysm images, we could identify similar aneurysms from databases of past cases. These extracted similar cases can support the decision-making process. In such way, neurosurgeons can base their judgement on past cases stored in database. According to feedbacks from neurosurgeons, the case-based reasoning can help them in two ways. One is to let them know the system is performing sensibly which increases their confidence in using it. Another is to give them an angle of view more intuitive than a single probability number that examines the current case from an overall statistical perspective. By comparing the current case with particular similar cases, the system provides a different angle of view to exploit past cases. Combining probability and past examples could provide a better picture for decision making. In our test with five neurosurgeons with different years of experience, most neurosurgeons' performances were significantly improved. It is worth noted that with the aid of the case-based reasoning, non-senior neurosurgeons could improve their performance to a level on par with that of seniors. This could be especially beneficial to health check-up centers or local hospitals that usually lack experienced neurosurgeons.

There are several limitations in our work. Manual segmentation of aneurysm is still required to obtain aneurysm mask as model input. In the future, we will incorporate automatic segmentation into our aneurysm rupture risk evaluation pipeline. Another limitation is that some clinical risk factors such as hyperlipidemia, hypertension, and smoking were not included due to unavailable data. The usefulness of case-based reasoning needs to be further validated with a larger number of cases and more neurosurgeons involved. The ratio of ruptured and stable cases is skewed which may bias the result. The prevalence in the current study is different from those reported in large cohort studies [2]; and therefore, the PPV and NPV should be interpreted carefully. The follow-up period of 2 years is relatively short; and thus, our result may not be fully applicable for predicting the long-term stability of aneurysms. Nevertheless, being able to estimate short-term to mid-term risk can still facilitate yearly regular monitoring of aneurysm status and treatment planning. The current study does not have external validation; and therefore, further validation using prospective, multi-center design with a larger number of cases recruited should be performed before our model's use in clinical practice.

Conclusions

Our proposed method enables the development of a competitive deep learning model using only a limited amount of data for aneurysm rupture prediction. A computer-aided diagnosis system with case-based reasoning was also developed and was shown to significantly improve neurosurgeons' performance in rupture prediction, which could be a potential tool for risk management of aneurysms.

Supplementary Information The online version contains supplementary material available at https://doi.org/10.1007/s00330-022-08608-7.

Funding Funding was provided through the National Natural Science Foundation of China under Grant (81974178, 81974177, U1813204, 61802385), and Shenzhen Fundmental Research Program under Grant (JCYJ20200109110208764, JCYJ20200109110420626).

Declarations

Guarantor The scientific guarantor of this publication is Chuan-Zhi Duan at Zhujiang Hospital.

Conflict of interest The authors of this manuscript declare no relationships with any companies whose products or services may be related to the subject matter of the article.

Statistics and biometry No complex statistical methods were necessary for this paper.

Informed consent Written informed consent was waived by the Institutional Review Board.

Ethical approval Approval for this study was obtained from the local Institutional Review Board of Macquarie University (MQ5201000234 and MQ5201950948228) and Zhujiang Hospital (2017-SJWK-007).

Methodology
- retrospective
- cross-sectional study
- performed at one institution

References

1. Li MH, Chen SW, Li YD et al (2013) Prevalence of unruptured cerebral aneurysms in Chinese adults aged 35 to 75 years: a cross-sectional study. Ann Intern Med 159:514–521. https://doi.org/10.7326/0003-4819-159-8-201310150-00004
2. Morita A, Kirino T, Hashi K et al (2012) The natural course of unruptured cerebral aneurysms in a Japanese cohort. New Engl J Med 366:2474–2482. https://doi.org/10.1056/NEJMoa1113260
3. Wiebers DO, Whisnant JP, Huston J 3rd et al (2003) Unruptured intracranial aneurysms: natural history, clinical outcome, and risks of surgical and endovascular treatment. Lancet. 362:103–110. https://doi.org/10.1016/s0140-6736(03)13860-3
4. Korja M, Kivisaari R, Rezai Jahromi B, Lehto H (2017) Natural history of ruptured but untreated intracranial aneurysms. Stroke. 48:1081–1084. https://doi.org/10.1161/STROKEAHA.116.015933
5. Xiang J, Natarajan SK, Tremmel M et al (2011) Hemodynamic-morphologic discriminants for intracranial aneurysm rupture. Stroke. 42:144–152. https://doi.org/10.1161/STROKEAHA.110.592923
6. Varble N, Tutino VM, Yu J et al (2018) Shared and distinct rupture discriminants of small and large intracranial aneurysms. Stroke. 49:856–864. https://doi.org/10.1161/STROKEAHA.117.019929
7. Cebral JR, Mut F, Weir J, Putman C (2011) Quantitative characterization of the hemodynamic environment in ruptured and unruptured brain aneurysms. AJNR Am J Neuroradiol 32:145–151. https://doi.org/10.3174/ajnr.A2419
8. Takao H, Murayama Y, Otsuka S et al (2012) Hemodynamic differences between unruptured and ruptured intracranial aneurysms during observation. Stroke. 43:1436–1439. https://doi.org/10.1161/STROKEAHA.111.640995
9. Zhang X, Karuna T, Yao ZQ et al (2019) High wall shear stress beyond a certain range in the parent artery could predict the risk of anterior communicating artery aneurysm rupture at follow-up. J Neurosurg 131:868–875. https://doi.org/10.3171/2018.4.JNS173179
10. Miura Y, Ishida F, Umeda Y et al (2013) Low wall shear stress is independently associated with the rupture status of middle cerebral artery aneurysms. Stroke. 44:519–521. https://doi.org/10.1161/STROKEAHA.112.675306
11. Tada Y, Wada K, Shimada K et al (2014) Roles of hypertension in the rupture of intracranial aneurysms. Stroke. 45:579–586. https://doi.org/10.1161/STROKEAHA.113.003072
12. Can A, Castro VM, Dligach D et al (2018) Lipid-lowering agents and high HDL (high-density lipoprotein) are inversely associated with intracranial aneurysm rupture. Stroke. 49:1148–1154. https://doi.org/10.1161/STROKEAHA.117.019972
13. Can A, Castro VM, Ozdemir YH et al (2018) Alcohol consumption and aneurysmal subarachnoid hemorrhage. Transl Stroke Res 9:13–19. https://doi.org/10.1007/s12975-017-0557-z
14. Can A, Castro VM, Ozdemir YH et al (2017) Association of intracranial aneurysm rupture with smoking duration, intensity, and cessation. Neurology. 89:1408–1415. https://doi.org/10.1212/WNL.0000000000004419
15. Juvela S (2019) Growth and rupture of unruptured intracranial aneurysms. J Neurosurg 131:843–851. https://doi.org/10.3171/2018.4.JNS18687
16. (2014) Development of the PHASES score for prediction of risk of rupture of intracranial aneurysms: a pooled analysis of six prospective cohort studies. Lancet Neurol 13:59–66
17. Bijlenga P, Gondar R, Schilling S et al (2017) PHASES score for the management of intracranial aneurysm a cross-sectional population-based retrospective study. Stroke. 48:2105–2112
18. Shi Z, Hu B, Schoepf UJ, et al (2020) Artificial intelligence in the management of intracranial aneurysms: current status and future perspectives. AJNR Am J Neuroradiol 41(3):373–379
19. Nakao T, Hanaoka S, Nomura Y et al (2018) Deep neural network-based computer-assisted detection of cerebral aneurysms in MR angiography. J Magn Reson Imaging 47:948–953
20. Stember JN, Chang P, Stember DM et al (2019) Convolutional neural networks for the detection and measurement of cerebral aneurysms on magnetic resonance angiography. J Digit Imaging 32:808–815
21. Sichtermann T, Faron A, Sijben R et al (2019) Deep learning–based detection of intracranial aneurysms in 3D TOF-MRA. AJNR Am J Neuroradiol 40:25–32
22. Ueda D, Yamamoto A, Nishimori M et al (2019) Deep learning for MR angiography: automated detection of cerebral aneurysms. Radiology 290:187–194
23. Park A, Chute C, Rajpurkar P et al (2019) Deep learning–assisted diagnosis of cerebral aneurysms using the HeadXNet model. JAMA Netw Open 2:e195600

24. Shi Z, Miao C, Schoepf UJ et al (2020) A clinically applicable deep-learning model for detecting intracranial aneurysm in computed tomography angiography images. Nat Commun 11(1):1–1
25. Yang J, Xie M, Hu C et al (2020) Deep learning for detecting cerebral aneurysms with CT angiography. Radiology. 3:192154
26. Dai X, Huang L, Qian Y et al (2020) Deep learning for automated cerebral aneurysm detection on computed tomography images. Int J Comput Assist Radiol Surg 13:1–9
27. Hu T, Yang H, Ni W et al (2020 Dec) Automatic detection of intracranial aneurysms in 3D-DSA based on a Bayesian optimized filter. Biomed Eng Online 19(1):1–8
28. Liu J, Chen Y, Lan L et al (2018) Prediction of rupture risk in anterior communicating artery aneurysms with a feed-forward artificial neural network. Eur Radiol 28:3268–3275
29. Detmer FJ, Lückehe D, Mut F et al (2019) Comparison of statistical learning approaches for cerebral aneurysm rupture assessment. Int J Comput Assist Radiol Surg 15:141–150
30. Liu Q, Jiang P, Jiang Y et al (2019) Prediction of aneurysm stability using a machine learning model based on PyRadiomics-derived morphological features. Stroke 50:2314–2321
31. Ou C, Chong W, Duan CZ, Zhang X, Morgan M, Qian Y (2021) A preliminary investigation of radiomics differences between ruptured and unruptured intracranial aneurysms. Eur Radiol 31(5):2716–2725
32. Silva MA, Patel J, Kavouridis V et al (2019) Machine learning models can detect aneurysm rupture and identify clinical features associated with rupture. World Neurosurg 131:e46–e51
33. Kim HC, Rhim JK, Ahn JH et al (2019) Machine learning application for rupture risk assessment in small-sized intracranial aneurysm. J Clin Med 8(5):683
34. Ahn JH, Kim HC, Rhim JK et al (2021) Multi-view convolutional neural networks in rupture risk assessment of small, unruptured intracranial aneurysms. J Pers Med 11(4):239
35. Heo J, Park SJ, Kang SH, Oh CW, Bang JS, Kim T (2020) Prediction of intracranial aneurysm risk using machine learning. Sci Rep 10(1):6921 1-0
36. Skodvin TO, Johnsen LH, Gjertsen O, Isaksen JG, Sorteberg A (2017) Cerebral aneurysm morphology before and after rupture: nationwide case series of 29 aneurysms. Stroke. 48(4):880–886
37. Wiebers DO (2003) International Study of Unruptured Intracranial Aneurysms Investigators. Unruptured intracranial aneurysms: natural history, clinical outcome, and risks of surgical and endovascular treatment. Lancet 362(9378):103–110
38. Japan Investigators UCAS (2012) The natural course of unruptured cerebral aneurysms in a Japanese cohort. N Engl J Med 366(26): 2474–2482
39. Ivantsits M, Goubergrits L, Kuhnigk JM et al (2022) Detection and analysis of cerebral aneurysms based on X-ray rotational angiography-the CADA 2020 challenge. Medical Image Analysis 77:102333
40. Timmins KM, van der Schaaf IC, Bennink E et al (2021) Comparing methods of detecting and segmenting unruptured intracranial aneurysms on TOF-MRAS: The ADAM challenge. NeuroImage 238:118216
41. Molinaro AM, Simon R, Pfeiffer RM (2005) Prediction error estimation: a comparison of resampling methods. Bioinformatics. 21: 3301–3307. https://doi.org/10.1093/bioinformatics/bti499
42. Demšar J (2006) Statistical comparisons of classifiers over multiple data sets. J Mach Learn Res 7(Jan):1–30
43. Xiang J, Yu J, Choi H et al (2015) Rupture Resemblance Score (RRS): toward risk stratification of unruptured intracranial aneurysms using hemodynamic–morphological discriminants. J Neurointerv Surg 7(7):490–495
44. Jiang P, Liu Q, Wu J et al (2018) A novel scoring system for rupture risk stratification of intracranial aneurysms: a hemodynamic and morphological study. Front Neurosci 12:596